

# Influence of adsorbate-substrate interaction on the local electronic structure of $C_{60}$ studied by low-temperature STM

C. Silien,<sup>\*</sup> N. A. Pradhan,<sup>†</sup> and W. Ho<sup>‡</sup>*Department of Physics and Astronomy and Department of Chemistry, University of California, Irvine, California 92697-4575, USA*

P. A. Thiry

*Laboratoire de Spectroscopie Moléculaire de Surface, Facultés Universitaires Notre-Dame de la Paix, B-5000 Namur, Belgium*

(Received 28 October 2003; revised manuscript received 21 January 2004; published 30 March 2004)

Low coverages of  $C_{60}$  on Cu(111) and K/Cu(111) have been investigated by scanning tunneling microscopy and spectroscopy at 10 K. By combining topographic imaging and mapping of the spectral intensity ( $dI/dV$ ), we have analyzed the evolution of the  $t_{1u}$ -derived [lowest-unoccupied molecular orbital (LUMO)] electronic states resulting from the difference in adsorption geometry on Cu(111) as well as the difference in bonding when the substrate is precovered by a K monolayer. The spatial distribution and the spectral width of the LUMO-derived states are observed to be particularly sensitive to the adsorbate-substrate interaction.

DOI: 10.1103/PhysRevB.69.115434

PACS number(s): 61.48.+c, 68.37.Ef, 68.43.Fg, 73.20.At

## I. INTRODUCTION

Soon after sizable quantities of  $C_{60}$  (Ref. 1) became available,<sup>2</sup> scanning tunneling microscopy (STM) unveiled important information about the interaction of the fullerene with surfaces. In particular, the resolution of bias-dependent internal features provided a direct visualization of the molecular orientations and gave a first insight into the geometry of various electronic states.<sup>3</sup> More recently, the measurement of  $dI/dV$  mappings of  $C_{60}/Ag(100)$  offered a better understanding of the spatial distribution of the molecular orbitals upon adsorption on a given substrate.<sup>4,5</sup> A very noticeable feature is the reported splitting of the  $C_{60}$  lowest-unoccupied molecular orbital (LUMO) into two dominant empty states of inverted geometry.<sup>4</sup> Theoretical investigations revealed that the observed spreading of the LUMO is a direct consequence of the interaction with silver.<sup>5</sup> The unique ability of STM to spatially resolve the electronic structure of adsorbates enabled the observation that the LUMO spectrum depends on the location of the molecules upon adsorption on Au(111) and Al(111).<sup>6,7</sup>

In order to further elucidate the role played by the substrate, we have analyzed the adsorption of  $C_{60}$  on Cu(111) and K/Cu(111). When deposited at room temperature, the fullerene chemisorbs on metals.<sup>8,9</sup> However, depending on the substrate, different degrees of hybridization and charge transfer are observed. On copper, the bond is thought to be predominantly ionic,<sup>9,10</sup> although hybridization occurs with the electronic states of the substrate.<sup>10,11</sup> Contrary to previous work performed on similar interfaces by averaging techniques, such as photoemission<sup>12,13</sup> and electron energy-loss spectroscopy,<sup>14,15</sup> we are able to distinguish different molecular orientations and locations on Cu(111) and to determine their effects on the molecular electronic structure. When  $C_{60}$  is deposited at low temperature on Cu(111) precovered by a K monolayer, we observe that ionic bonds are established with the K atoms. By comparing both systems, we are able to study the influence of adsorbate-substrate interaction on the electronic structure of  $C_{60}$ .

## II. EXPERIMENTAL ARRANGEMENT AND SAMPLE PREPARATION

For the STM measurements, we used a homemade, variable-temperature microscope in ultrahigh vacuum (UHV), built according to a previously detailed design.<sup>16</sup> The experiments were performed at 10 K under a pressure of  $2 \times 10^{-11}$  Torr. The  $dI/dV$  data were measured through lock-in detection of the alternating tunneling current driven by modulating the sample bias ( $\sim 10$  mV,  $\sim 200$  Hz) with the feedback loop open. The Cu(111) substrate was cleaned in UHV by repeated cycles of  $Ne^+$  sputtering and annealing around 850 K.  $C_{60}$  (99.9% purity, Aldrich) was sublimated from an alumina crucible and K from a commercial source (SAES Getter). The microscope design allows *in situ* dosing at any temperature ranging from about 350 K down to 10 K.  $C_{60}$  was dosed at room temperature (RT) on the clean Cu(111). On the K precovered surface, the fullerene was deposited at 10 K in order to avoid any strong interaction with the underlying copper, while the ordered K monolayer was grown at RT before cooling the sample down.

## III. RESULTS

### A. Adsorption on Cu(111)

When dosed at room temperature on Cu(111),  $C_{60}$  monolayers start growing from the step edges, as a result of molecular diffusion, and the molecules are expected to occupy threefold hollow sites.<sup>3</sup> The topography recorded in constant-current mode and presented in Fig. 1 was measured close to a step edge of the Cu(111) surface. The first image was recorded with the sample bias set at +2.0 V relative to the tip [Fig. 1(a)]. According to previous investigations, the intramolecular features are localized on the pentagons forming the  $C_{60}$  skeleton.<sup>3-6,17</sup> The second image was recorded at +0.7 V [Fig. 1(b)]. The intramolecular features should be representative of other electronic states but are still partially localized on the pentagons. For clarity, a map of the different domains is shown in Fig. 1(c). In agreement with previous results,<sup>3</sup> most of the molecules are adsorbed on the lower

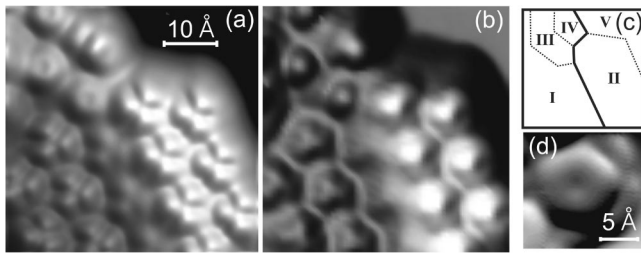


FIG. 1. Constant current (0.1 nA) topographic images of a  $C_{60}$ -covered area of Cu(111), recorded in the vicinity of a step edge, (a) +2.0 V and (b) +0.7 V. Both images have been filtered for clarity. A map of the same location is drawn in (c) and is divided into five areas. The continuous line crossing the map indicates the step edge; areas II and V are situated on the upper terrace side. A closeup of one molecule adsorbed with a pentagon facing up is shown in (d). That latter image was recorded at +2.0 V.

terrace along the step edge and possess a clear threefold symmetry (clover shape, area I). As three pentagons should be connected by one hexagon in  $C_{60}$ , the clover-shaped molecules are adsorbed with a hexagon facing up and the opposite hexagon lying on the copper, parallel to the surface.

A small number of molecules are found on the upper terrace along the step edge (i.e., the seven brightly imaged molecules in area II). Such molecular positions have not been reported before and could result from the absence of any postdeposition annealing in our experiment. Although we cannot completely rule it out, the presence of an impurity that would trap one molecule and allow the growth of an island around it appears unlikely. Indeed, none of these seven molecules is randomly oriented as is observed when  $C_{60}$  are actually trapped by impurities. The latter is probably the case for the single molecule in area IV. In addition, all the seven molecules show the same  $dI/dV$  curves, indicating none of them is particularly perturbed [see below, Fig. 2(b)]. At room temperature,  $C_{60}$  are expected to migrate and eventually get trapped on the lower terrace along step edges or by other  $C_{60}$  molecules, leading to monolayer growth. However, because of a competition between the  $C_{60}$ - $C_{60}$  and  $C_{60}$ -Cu interactions, it is also possible that the molecules find favorable locations on the upper terrace of a decorated step edge, whose height is much smaller than the  $C_{60}$  diameter. Three  $C_{60}$  adsorbed with a pentagon facing up are also visible in the image (area III). This orientation is not common on Cu(111) but has been observed on other substrates, e.g., Ag(111).<sup>18</sup> A closeup of a molecule is shown in Fig. 1(d) and testifies the fivefold symmetry of the pentagon.

Three different adsorbed species are thus reported here for  $C_{60}$  dosed at room temperature on Cu(111):  $C_{60}$  adsorbed on lower terraces with a hexagon parallel to the surface (area I),  $C_{60}$  on upper terraces (area II), and  $C_{60}$  with a pentagon facing up (area III). Even though the topographical images do not show important differences between them, the three species have different spectroscopic behavior that has been carefully analyzed by recording the voltage dependence of the  $dI/dV$  intensity and by imaging its spatial dependence at particular bias values.

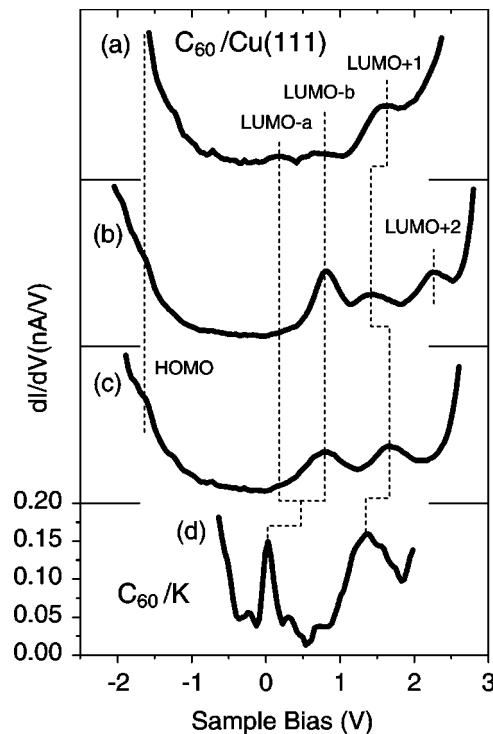


FIG. 2. Typical  $dI/dV$  curves recorded at the center of  $C_{60}$  molecules. Spectra (a)–(c) were recorded over  $C_{60}$  on Cu(111): (a) clover-shaped  $C_{60}$  on the lower terrace, (b) clover-shaped  $C_{60}$  on the upper terrace, and (c)  $C_{60}$  with a pentagon facing up. Spectra (a)–(c) were measured with the tip height set at 0.1 nA and +2.0 V. (d) A set point of 0.1 nA and +1.5 V was used for the spectrum of  $C_{60}$  adsorbed on K/Cu(111).

Typical  $dI/dV$  vs  $V$  spectra are shown in Fig. 2: (a) over a molecule in area I, (b) in area II, and (c) in area III. A strong spatial inhomogeneity within the molecules is also observed and is shown below by the  $dI/dV$  images. These spectra were recorded with the same tip positioned over the center of the molecules. Four main features appear in the spectra: a peak at  $1.66 \pm 0.1$  V (LUMO+1), a peak at  $0.77 \pm 0.1$  V (LUMO- $b$ ), a small peak or shoulder at  $0.19 \pm 0.1$  V (LUMO- $a$ ), and a barely visible shoulder around  $-1.65$  V [highest-occupied molecular orbital (HOMO)]. In agreement with previous studies,<sup>4–6,19,20</sup> we propose that these peaks are derived from the  $t_{1g}$ ,  $t_{1u}$ , and  $h_u$  molecular orbitals of  $C_{60}$  that, respectively, correspond to the LUMO+1, the LUMO, and the HOMO of the isolated molecules. Both the LUMO- $a$  and the LUMO- $b$  peaks are expected to derive from the  $t_{1u}$  orbital.<sup>4,5</sup> For the  $C_{60}$  adsorbed on the upper terrace (b), the LUMO+1 peak is measured at  $1.50 \pm 0.1$  V, while another one, assigned to a  $h_g$ -derived molecular level, is observed at  $2.20 \pm 0.1$  V (LUMO+2). The relative intensities and energies of these peaks are characteristic of the adsorption site.

The  $dI/dV$  images provide substantial information about the spatial distribution of the molecular electronic states. We will now analyze two selected areas of the sample. A topography of the first area recorded at +1.65 V is shown in Fig. 3(a). All molecules are lying on the lower terrace along a step edge. Three molecules with a pentagon facing up are

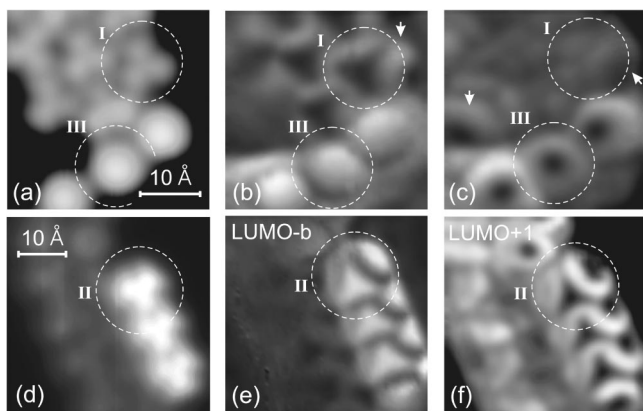


FIG. 3. (a) and (d) Constant current topographic images (0.1 nA, +1.65 V) of two  $C_{60}$ -covered areas of Cu(111). (b) and (e) Corresponding  $dI/dV$  images of the LUMO- $b$  peak (+0.7 V), (c) and (f) LUMO+1 peak (+1.65 V).

observed (round shape, i.e., molecule III). The other molecules are adsorbed with a hexagon facing up (clover shape, i.e., molecule I). In the topography of the second area [Fig. 3(d)], three molecules (clover shape, i.e., molecule II) are seen to be trapped on the upper terrace along a step edge. For both areas,  $dI/dV$  images representative of LUMO- $b$  and LUMO+1 electronic states are presented. These images were recorded with bias values of +0.7 and +1.65 V, respectively.

For the clover-shaped molecules, located on the lower terrace, the spatial distribution of the LUMO- $b$  resembles bright hollow triangles whose edges are parallel to the surface (molecule I). Comparison with the topography leads to the conclusion that these edges fit the pentagon-hexagon bonds and that the dark part is centered on the top hexagonal face of  $C_{60}$ . In agreement with early theoretical simulations of the charge density of the LUMO of  $C_{60}$ ,<sup>17</sup> the molecules trapped at the border of the island reveal that the signal at the edge is distributed over the entire pentagon rings next to the top hexagon of each  $C_{60}$  [identified by the white arrow in Fig. 3(b)]. For molecules adsorbed with a pentagon facing up, the LUMO- $b$  signal appears as a bright feature centered on the pentagon (molecule III). Interestingly, this particular distribution cannot be accounted for by simply considering the change in the  $C_{60}$  orientation between clover- and round-shaped molecules but suggests the existence of differences in the electronic structure of the molecules. This second distribution is, however, compatible with the one measured when fullerenes are trapped on the upper terrace (molecule II), where the LUMO- $b$  spatial distribution also appears inverted compared to the one observed when the clover-shaped molecules are located on the lower terrace. Indeed, the previously dark triangle centered on the hexagon becomes bright, along with strong signals at the center of the pentagons bordering the top hexagon of each  $C_{60}$ .

The  $dI/dV$  images suggest that the actual orientation of the molecules with respect to the substrate changes when the  $C_{60}$  are located on lower or upper terraces. On the lower terraces, the threefold symmetry axis passing through the top hexagon of the  $C_{60}$  molecules is perpendicular to the sub-

strate so that these molecules should adsorb with a hexagon parallel to the surface (molecule I). However, the symmetry axis appears slightly tilted when the molecules are trapped on the upper terrace (molecule II), suggesting that these  $C_{60}$  may not adsorb with a hexagon perfectly parallel to the copper surface. If true, such a tilt could be explained by the copper height difference that needs to be compensated in order to accommodate the interaction between the  $C_{60}$  adsorbed on the upper and lower terraces, causing the fullerenes to face each other with a specific orientation as in the rotationally inhibited phase of bulk  $C_{60}$ .<sup>21</sup> Given that a similar tilt is also observed when two rows of molecules are trapped on upper terraces, we rule out any artifact that could occur when imaging the border of a  $C_{60}$  island. Because the same observation was made when using different tips, the influence of tip geometry can be ruled out as well. However, the possible change in the molecular orientation is not absolutely clear from the topography. Nevertheless, the important differences observed in the LUMO- $b$  spatial distribution as a function of the molecular orientation or location indicate that the subsequent changes in bonding play a crucial role in the establishment of the electronic structure at the interface.

Two LUMO-derived components were also detected at the  $C_{60}/\text{Ag}(100)$  interface,<sup>4,5</sup> labeled LUMO- $a$  and - $b$  in our discussion of  $C_{60}/\text{Cu}(111)$ . On silver, the spatial distributions of these two electronic states are roughly inverted and the LUMO- $b$  distribution is similar to our observation when the molecules are adsorbed with a pentagon facing up or on the upper terraces. However, the results do not depend on the molecular orientation or location on  $\text{Ag}(100)$ .<sup>4,5</sup> On Cu(111), the LUMO- $a$  peak intensity is much smaller (Fig. 2) than on  $\text{Ag}(100)$  and could not be mapped satisfactorily. On the contrary, the LUMO+1 can be easily imaged here. In contrast to the LUMO- $b$  state, its spatial intensity is independent of the  $C_{60}$  orientation and position on the surface, suggesting a different type of interaction between this electronic level and the substrate. We observe that the intensity of the LUMO+1 is once again distributed on the pentagonal rings of  $C_{60}$ . This is particularly clear for the molecules trapped on the upper terrace (molecule II), oriented with a pentagon facing up (molecule II), and the clover-shaped  $C_{60}$  located at the border of the island on the lower terrace [see white arrows in Fig. 3(c)]. For the other molecules, the signal appears like three bright features (molecule I) and not hollow triangles as for the LUMO- $b$ . Topographical images indicate that the actual tip trajectories are different for the  $dI/dV$  images recorded at +0.7 and +1.65 V. The tip displacement is known to play a role in the appearance of such images<sup>5</sup> and, to some extent, it could explain the differences between the LUMO- $b$  and LUMO+1 for that adsorption geometry. However, it is also possible that these differences in the patterns truly reflect variations in the spatial distribution of these two electronic states. In any case, the LUMO+1 measured here agrees well with the distribution measured on  $C_{60}/\text{Ag}(100)$ <sup>4,5</sup> and testifies that the LUMO components are the electronic states affected the most upon adsorption.

### B. Adsorption on K precovered Cu(111)

Many studies have focused on the growth of alkali-metal layers on metal surfaces and more particularly on the adsorp-



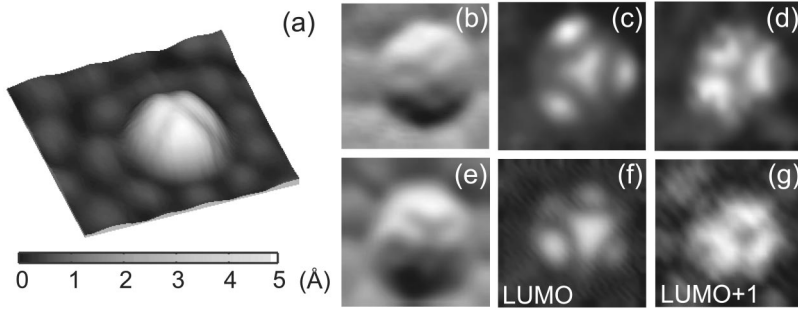


FIG. 4. (a) Constant current three-dimensional topography (0.1 nA, +1.5 V,  $44 \times 44 \text{ \AA}^2$ ) of one isolated C<sub>60</sub> adsorbed on a K precovered Cu(111) crystal at 10 K. The C<sub>60</sub> adsorbs with a hexagon facing up and is surrounded by nine K atoms. (b) and (e) Topographic images (0.1 nA, +1.3 V,  $30 \times 30 \text{ \AA}^2$ ) of two isolated C<sub>60</sub> molecules on K/Cu(111). (c) and (f) Corresponding  $dI/dV$  images at +0.04 V (LUMO), and (d) and (g) +1.3 V (LUMO+1).

tion of K on Cu(111) (Ref. 22, and references therein). When potassium is dosed on Cu(111) at liquid-nitrogen temperature, an incommensurate hexagonal lattice is formed. Due to the small lateral energy variation for alkali metals on Cu(111), the layer density continuously increases with dosing, up to a saturation coverage for which a nearest-neighbor (NN) spacing between atoms of about 4.4 Å is reported.<sup>22</sup> Although in our experiment the K monolayer was grown at room temperature and measured at 10 K, we observed very similar behavior, except that the second-layer islands were already seen for a first-layer coverage corresponding to a NN distance of  $\sim 8.0 \text{ \AA}$ . The alkali-metal/Cu(111) interfaces possess quantum well (QW) states resulting from the electronic confinement at the surface.<sup>23</sup> The QW states appear as strong peaks in  $dI/dV$  curves recorded above the alkali-metal layer. The energy of the first QW level depends on the density of the K layer. The density can consequently be chosen so that no QW states are present in the expected energy range of the C<sub>60</sub> electronic states. We used K monolayers of about  $11.5 \pm 0.5 \text{ \AA}$  NN distance for which the first QW level is recorded at about +2.6 V. By comparison, the first QW level appears at +1.7 V when the NN separation is  $8.0 \pm 0.5 \text{ \AA}$ .

When dosed at 10 K onto K precovered Cu(111), C<sub>60</sub> molecules are relatively stable because of the formation of ionic bonds with the alkali-metal atoms. Almost no migration can be observed when small tunneling currents are used (e.g., 0.1 nA) and the molecules are adsorbed with a hexagon facing up (clover-shaped molecules) and surrounded by nine K atoms [see Fig. 4(a)]. On a hexagonal K surface, the STM topographic image can be accounted for if the C<sub>60</sub> occupies a threefold hollow site and stands on top of three alkali-metal atoms. After long measurements the nine surrounding K atoms eventually assumed different positions, suggesting that their interaction with C<sub>60</sub> is negligible, and some C<sub>60</sub> molecules are slightly rotated [e.g., see Fig. 4(e)] and displaced. These changes can be understood as resulting from a local rearrangement of the K atoms underneath the molecule, which is very likely due to the small lateral variation of the potential energy felt by K on Cu(111).

A typical  $dI/dV$  curve recorded over a C<sub>60</sub> molecule is shown in Fig. 2(d). Two peaks of molecular origin are detected and labeled LUMO and LUMO+1. They are observed at  $0.03 \pm 0.03$  and  $1.4 \pm 0.1 \text{ V}$ , respectively. Their typical widths are around 0.15 and 0.6 V. The LUMO width is therefore three or four times smaller than the one observed for C<sub>60</sub>/Cu(111), while the LUMO+1 width does not differ. Given that the energy of the electronic states should reflect

the charge transfer to C<sub>60</sub>, we infer that the K layer donates around three electrons to the fullerene molecule. The LUMO peak is indeed located very close to the Fermi level, which suggests that the electronic state is almost half filled. The transferred charges can be obtained from the K atoms directly below the C<sub>60</sub>, in line with previous photoemission results.<sup>24</sup> Because of the charge transfer and the absence of interaction with the copper atoms underneath, C<sub>60</sub> is expected to be ionically bonded to K/Cu(111).

$dI/dV$  mappings of these electronic states are shown in Fig. 4 for two different isolated molecules. Although it crosses the Fermi level, the LUMO peak [Figs 4(c) and 4(f)] has similar spatial distribution as the LUMO-*b* on C<sub>60</sub>/Cu(111) when the molecules are adsorbed on upper terraces or oriented with a pentagon facing up. However, the actual LUMO pattern for C<sub>60</sub>/K/Cu(111) does not depend here on the molecular adsorption geometry as demonstrated by comparing Figs. 4(c) and 4(f). When imaged, the LUMO+1 shows similar distribution as measured on Cu(111), indicating little effect of K on that orbital [Figs 4(d) and 4(g)].

#### IV. DISCUSSION

Theoretical evaluations of the charge density of various C<sub>60</sub> electronic states are available in the literature. First-principles band calculations of C<sub>60</sub> monolayers on Cu(111) have been performed, without considering any interactions between the substrate and the fullerene, e.g., charge transfer and mixing of electronic levels.<sup>17</sup> There, the role of copper is limited to the determination of the adsorption structure in the monolayer. Such computation shows almost no spreading of the  $t_{1u}$ -derived states and indicates that the associated charge distribution is localized on the pentagonal rings. More recently, local-density calculations have been performed for isolated C<sub>60</sub> molecules adsorbed on Ag(100).<sup>5</sup> The experimentally observed spreading of the LUMO-derived state is reproduced when the silver substrate is explicitly taken into account. With such a model, the charge distribution at the Fermi level is also localized on the pentagonal rings. However, at higher energy (+0.4 V), the distribution is roughly inverted, as in the experiment.<sup>4,5</sup> Therefore, it is clear that the substrate plays a crucial role in determining the actual electronic structure of adsorbed C<sub>60</sub>.

We observed that the  $dI/dV$  images of the dominant LUMO-derived states are quite similar upon adsorption on Cu(111) (molecules on upper terraces or oriented with a pentagon facing up), Ag(100), and K/Cu(111). Because only

ionic bonds between  $C_{60}$  and K atoms are expected on K/Cu(111), it is tempting to conclude that charge transfer plays a significant role in all these systems. However, it is clear that charge transfer alone is unable to explain all the features detected by the spectroscopic analysis. In accordance with the calculations,<sup>5</sup> the observation of only one particularly narrow component deriving from the  $t_{1u}$  orbital for  $C_{60}$ /K/Cu(111) is attributed to the absence of strong interaction with the copper substrate. On Cu(111), the electronic level mixing between copper and carbon atoms is likely to affect the electronic structure of the interfaces and may also account for the difference in the  $dI/dV$  patterns of the LUMO- $b$  as a function of the adsorption geometry. Hence, on the lower terrace, the particular bonding conditions characterized by the occupation of threefold hollow sites of Cu(111) and the adsorption with a hexagon parallel to the surface may cause the empty LUMO-derived state at +0.7 V (LUMO- $b$ ) to possess a particular spatial distribution.

## V. CONCLUSIONS

To summarize, we have analyzed the electronic structure of  $C_{60}$  adsorbed on Cu(111) before and after precovering the substrate by a monolayer of K. On Cu(111), the LUMO is split into two states while only one narrow electronic state is

observed on K/Cu(111). Their spatial distributions have been analyzed by recording  $dI/dV$  images. We have demonstrated that the charge distribution of  $C_{60}$  on Cu(111) strongly depends on the molecular location and orientation with respect to the substrate. Comparison of the local electronic structures of  $C_{60}$ /Cu(111) and  $C_{60}$ /K/Cu(111) further highlights the role of the adsorbate-substrate interaction, leading to charge transfer and mixing of electronic levels.

## ACKNOWLEDGMENTS

This paper is based upon work supported by the Chemical Science, Geo- and Bioscience Division, Office of Science, U.S. Department of Energy under Grant No. DE-FG03-01ER15157. The authors are grateful to Dr. J.R. Ahn for his valuable help with the experimental development and to Professor P. Lambin, Professor P. Rudolf, and Dr. Y. Caudano for fruitful discussions. In addition, C.S. acknowledges a grant from the French Community of Belgium and financial support from the CERUNA Belgian foundation, the Belgian National Fund for Scientific Research (FNRS), and the Belgian Interuniversity Program on "Quantum Size Effects in Nanostructured Materials" PAI/IUAP 5/1 initiated by the Belgian Office for Scientific, Technical and Cultural Affairs (OSTC).

\*On leave from Laboratoire de Spectroscopie Moléculaire de Surface, Facultés Universitaires Notre-Dame de la Paix, B-5000 Namur, Belgium.

†On leave from Department of Physics, Cornell University, Ithaca, NY 14853-2501, USA.

‡Electronic address: wilsonho@uci.edu

<sup>1</sup>H.W. Kroto, J.R. Heath, S.C. O'Brian, R.F. Curl, and R.E. Smalley, *Nature* (London) **318**, 162 (1985).

<sup>2</sup>W. Krätschmer, L.D. Lamb, K. Fostiropoulos, and D.R. Huffman, *Nature* (London) **347**, 354 (1990).

<sup>3</sup>T. Hashizume, K. Motai, X.D. Wang, H. Shinohara, Y. Saito, Y. Maruyama, K. Ohno, Y. Kawazoe, Y. Nishina, H.W. Pickering, Y. Kuk, and T. Sakurai, *Phys. Rev. Lett.* **71**, 2959 (1993).

<sup>4</sup>M. Grobis, X. Lu, and M.F. Crommie, *Phys. Rev. B* **66**, 161408 (2002).

<sup>5</sup>X. Lu, M. Grobis, K.H. Khoo, S.G. Louie, and M.F. Crommie, *Phys. Rev. Lett.* **90**, 096802 (2003).

<sup>6</sup>C. Rogero, J.I. Pascual, J. Gomez-Herrero, and A.M. Baro, *J. Chem. Phys.* **116**, 832 (2002).

<sup>7</sup>M.K.-J. Johansson, A.J. Maxwell, S.M. Gray, P.A. Brühwiler, D.C. Mancini, L.S.O. Johansson, and N. Mårtensson, *Phys. Rev. B* **54**, 13 472 (1996).

<sup>8</sup>P. Rudolf, in *Fullerenes and Fullerene Nanostructures*, edited by J. Fink, M. Mehring, and S. Roth (World Scientific, Singapore, 1996), p. 263.

<sup>9</sup>A.V. Hamza, in *Fullerenes: Chemistry, Physics, and Technology*, edited by K.M. Kadish and R.S. Ruoff (Wiley, New York, 2000), p. 531.

<sup>10</sup>A.J. Maxwell, P.A. Brühwiler, D. Arvanitis, J. Hasselström,

M.K.-J. Johansson, and N. Mårtensson, *Phys. Rev. B* **57**, 7312 (1998).

<sup>11</sup>B.W. Hoogenboom, R. Hesper, L.H. Tjeng, and G.A. Sawatzky, *Phys. Rev. B* **57**, 11 939 (1998).

<sup>12</sup>K.-D. Tsuei, J.-Y. Yuh, C.-T. Tzeng, R.-Y. Chu, S.-C. Chung, and K.-L. Tsang, *Phys. Rev. B* **56**, 15 412 (1997).

<sup>13</sup>K.-D. Tsuei and P.D. Johnson, *Solid State Commun.* **101**, 337 (1997).

<sup>14</sup>M.R.C. Hunt, P. Rudolf, and S. Modesti, *Phys. Rev. B* **55**, 7882 (1997).

<sup>15</sup>C. Silien, I. Marenne, J. Auerhammer, N. Tagmatarchis, K. Prasad, P.A. Thiry, and P. Rudolf, *Surf. Sci.* **482-485**, 1 (2001).

<sup>16</sup>B.C. Stipe, M.A. Rezaei, and W. Ho, *Rev. Sci. Instrum.* **70**, 137 (1999).

<sup>17</sup>Y. Maruyama, K. Ohno, and Y. Kawazoe, *Phys. Rev. B* **52**, 2070 (1995).

<sup>18</sup>E.I. Altman and R.J. Colton, *Phys. Rev. B* **48**, 18 244 (1993).

<sup>19</sup>A.W. Dunn, E.D. Svensson, and C. Dekker, *Surf. Sci.* **498**, 237 (2002).

<sup>20</sup>X. Yao, T.G. Ruskell, R.H. Workman, D. Sarid, and D. Chen, *Surf. Sci.* **366**, L743 (1996).

<sup>21</sup>M. S. Dresselhaus, G. Dresselhaus, and P.C. Eklund, *Science of Fullerenes and Carbon Nanotubes* (Academic Press, New York, 1996).

<sup>22</sup>R.D. Diehl and R. McGrath, *Surf. Sci. Rep.* **23**, 43 (1996).

<sup>23</sup>G. Hoffmann, J. Klier, and R. Berndt, *Phys. Rev. Lett.* **87**, 176803 (2001).

<sup>24</sup>L.Q. Jiang and B.E. Koel, *Phys. Rev. Lett.* **72**, 140 (1994).